

Early Progress on Lower-Noise Fabrication Development for the Future, Full-Scale Advantage2 Quantum Computer

WHITEPAPER

Summary

The experimental, small-scale Advantage2™ prototype launched in June 2022 was developed in our current rapid-development fabrication stack, while the eventual full-scale Advantage2 product will be produced in an all-new lower-noise stack. Here we compare the fabrication stack used for the Advantage2 prototype chip to the improved stack in development for the Advantage2 product. We find a 7× reduction in $1/f$ noise at 1 Hz, a 3× reduction in integrated flux noise, and over an order of magnitude reduction in high-frequency flux noise near 2 GHz. These significant noise reductions should lead to significant performance gains in the eventual full-scale Advantage2 system.

1 Overview

The growing evidence of computational advantage for coherent annealing [1, 2] in experiments with short anneal times makes clear the need for increasing the coherence of quantum annealers. While D-Wave’s previous demonstrations of coherent annealing have shown a path toward performance improvements, they have relied on extremely short anneal times that are difficult to implement on production systems. Another path toward practical coherent quantum annealing is to reduce the noise intrinsic to the materials set and fabrication processes used to make our processors. D-Wave implements its qubits in a multi-layer superconducting integrated circuit fabrication stack of alternating conducting and insulating layers, referred to hereafter as “stack” for simplicity. Reducing noise in our stack is desirable for improving the high-performance, high-connectivity quantum processing units (QPUs) needed for practical quantum computing.

D-Wave has a long history of measuring and reducing noise in superconducting flux qubits [3–8]. Here, we compare flux noise in our rapid-development stack FAB-A to our lower-noise stack FAB-B. The small-scale Advantage2 prototype processor was developed in the FAB-A stack, but the eventual full-scale Advantage2 product will be produced in a stack similar to the new FAB-B stack. We measure noise in these two stacks using flux qubits with the same geometry and shielding configuration used in our Advantage QPUs. We find that FAB-B yields a 7× reduction in $1/f$ flux noise at 1 Hz, a 3× reduction in integrated flux noise, and over an order of magnitude reduction in high-frequency flux noise near 2 GHz when compared to FAB-A. Because the Advantage2 qubit geometry is different from the Advantage qubit geometry due to Advantage2’s higher connectivity, the absolute noise numbers will be different than reported here. However, the relative drop in flux noise reported here should apply directly between the small-scale Advantage2 prototype and the full-scale Advantage2 product.

2 $1/f$ Flux Noise

Low-frequency flux noise is directly measured by taking the power spectral density of a time stream of flux offset measurements [4, 6]. We fit the results to a simple $1/f$ noise model, $S_{\Phi} = A_{1/f}^2 (f/1 \text{ Hz})^{-\alpha} + w_n$, where $A_{1/f}$ is the amplitude of the noise, α is the slope of the spectrum, and w_n is the white noise background. We measured this across several devices from each stack. Data from two devices is shown for comparison in Figure 1, and the $1/f$ noise measurement results are summarized in Table 1. $1/f$ noise at 1 Hz has dropped by a factor of 7 in the new FAB-B stack.

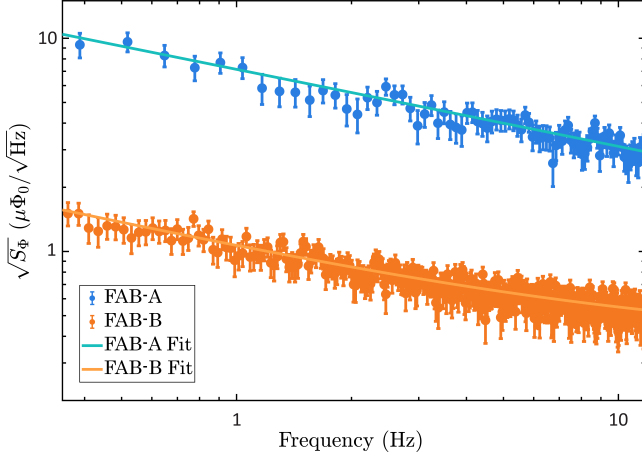


Figure 1: Example $1/f$ measurements of devices from the two stacks.

| Stack | $A_{1/f}$ ($\mu\Phi_0/\sqrt{\text{Hz}}$) | α |
|-------|--|-----------------|
| FAB-A | 7.2 ± 0.2 | 0.72 ± 0.02 |
| FAB-B | 1.0 ± 0.1 | 0.80 ± 0.02 |

Table 1: Comparison of $1/f$ flux noise in the two stacks.

3 Broadband Flux Noise

Macroscopic resonant tunneling (MRT) is an efficient way to measure integrated and high-frequency flux noise in DC-SQUID-like qubits. We sweep our qubit flux bias ϵ approximately across the qubit frequency range 0.1-5 GHz, and measure the lowest-order MRT peak width W_{MRT} . We also fit the high-frequency flux noise tail on the MRT peak, which has traditionally been reported as the dimensionless parameter η [5, 9]. However, this particular metric is not easily comparable across different qubit designs, so we have developed a magnetic loss tangent $\tan \delta^L(\omega)$ similar to those developed by others [10]. It can be thought of as the inductive version of the dielectric loss tangent $\tan \delta^C(\omega)$, with the internal quality factor Q_i of an LC resonator driven at resonance ω_0 defined as $1/Q_i = \tan \delta^L(\omega_0) + \tan \delta^C(\omega_0)$, where $\tan \delta^L = P_{\text{diss}}^L / \omega_0 2E_{\text{stored}}^L$, $\tan \delta^C = P_{\text{diss}}^C / \omega_0 2E_{\text{stored}}^C$, P_{diss}^L (P_{diss}^C) is the total inductive (capacitive) energy dissipated in the resonator per unit time, and E_{stored}^L (E_{stored}^C) is the inductive (capacitive) energy stored. $\tan \delta^L(\omega)$ can be expressed as part of the high-frequency flux noise spectral density $S_{\text{HF}} = 2\hbar L \frac{\tan \delta^L(\omega)}{1 - e^{-\hbar\omega/k_B T}}$ for a qubit with inductance L ,

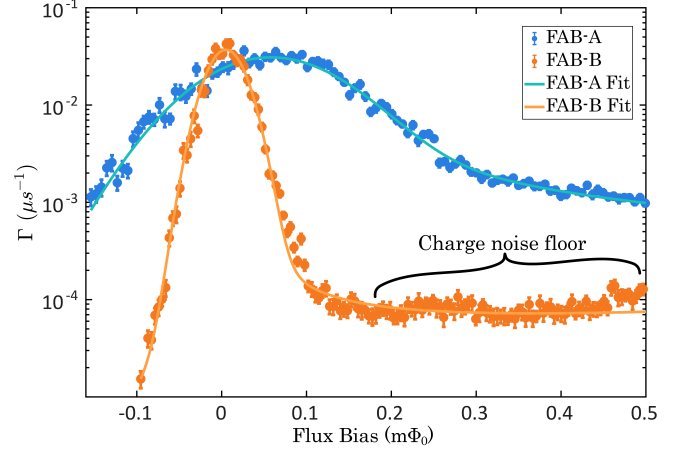


Figure 2: Example MRT peak measurements of devices from the two stacks. The charge noise floor limits the resolution of the $\tan \delta^L$ fit of FAB-B.

and only needs to be scaled by the device frequency to compare between qubit designs.

A comparison of representative MRT peaks from both stacks are shown in Figure 2, where Γ is the inter-well tunneling rate, and Table 2 is a summary of the MRT noise measurement results. While the integrated flux noise has dropped by a factor of more than $3\times$, the biggest gain for FAB-B is the more than order of magnitude reduction in high-frequency flux noise. It should be noted that the measurement noise floor, set by the device charge noise[11], largely dominates the $\tan \delta^L$ measurement in the FAB-B devices. This leads to large error bars in the $\tan \delta^L$ fitting, and suggests that the next target for FAB-B should be reduced charge noise. The $\tan \delta^L$ result is reported at 2 GHz.

| Stack | W_{MRT} ($\mu\Phi_0$) | $\tan \delta^L$ | η |
|-------|----------------------------------|------------------------------|-------------------|
| FAB-A | 73.4 ± 0.4 | $(104 \pm 4) \times 10^{-6}$ | 0.433 ± 0.080 |
| FAB-B | 21.4 ± 0.3 | $(7 \pm 3) \times 10^{-6}$ | 0.023 ± 0.010 |

Table 2: Comparison of integrated flux noise in the two stacks. $\tan \delta^L$ is reported at 2 GHz.

4 Conclusion

We have previously seen that even modest decreases in noise can lead to dramatic improvements in performance on spin

glass problems [7, 8]. As a significant step towards delivering higher-coherence quantum annealing processors to our customers, we have demonstrated a significantly lower-noise stack compared to the small-scale Advantage2 prototype stack. This lower-noise stack is very similar to the stack that will be used in the eventual full-scale Advantage2 quantum computer. Therefore, the $7\times$ lower $1/f$ flux noise at 1 Hz, $3\times$ lower integrated flux noise, and order of magnitude decrease in high-frequency flux noise measured here should persist into the Advantage2 product. Additionally, we find that charge noise now dominates the individual qubit high-frequency noise (~ 2 GHz), and sets a clear target for further improvement in future products.

References

- ¹ A. D. King, J. Raymond, T. Lanting, S. V. Isakov, M. Mohseni, et al., “Scaling advantage over path-integral Monte Carlo in quantum simulation of geometrically frustrated magnets,” *Nat Commun* **12**, 1113 (2021).
- ² A. D. King, S. Suzuki, J. Raymond, A. Zucca, T. Lanting, et al., “Coherent quantum annealing in a programmable 2000-qubit Ising chain,” (2022) [10.48550/ARXIV.2202.05847](https://arxiv.org/abs/2202.05847).
- ³ R. Harris, M. W. Johnson, S. Han, A. J. Berkley, J. Johansson, et al., “Probing noise in flux qubits via macroscopic resonant tunneling,” *Phys. Rev. Lett.* **101**, 117003 (2008).
- ⁴ T. Lanting, A. J. Berkley, B. Bumble, P. Bunyk, A. Fung, et al., “Geometrical dependence of the low-frequency noise in superconducting flux qubits,” *Phys. Rev. B* **79**, 060509 (2009).
- ⁵ T. Lanting, M. H. S. Amin, M. W. Johnson, F. Altomare, A. J. Berkley, et al., “Probing high-frequency noise with macroscopic resonant tunneling,” *Phys. Rev. B* **83**, 180502 (2011).
- ⁶ T. Lanting, M. H. Amin, A. J. Berkley, C. Rich, S-F. Chen, S. LaForest, and R. de Sousa, “Evidence for temperature-dependent spin diffusion as a mechanism of intrinsic flux noise in SQUIDS,” *Phys. Rev. B* **89**, 014503 (2014).
- ⁷ *Whitepaper: Probing Mid-Band and Broad-Band Noise in Lower-Noise D-Wave 2000Q Fabrication Stacks*, tech. rep. 14-1034A-A (D-Wave Systems Inc., 2019).
- ⁸ *Whitepaper: Improved coherence leads to gains in quantum annealing performance*, tech. rep. 14-1037A-A (D-Wave Systems Inc., 2019).
- ⁹ A. J. Leggett, S. Chakravarty, A. T. Dorsey, M. P. A. Fisher, A. Garg, and W. Zwerger, “Dynamics of the dissipative two-state system,” *Rev. Mod. Phys.* **59**, 1–85 (1987).
- ¹⁰ L. B. Nguyen, Y.-H. Lin, A. Somoroff, R. Mencia, N. Grabon, and V. E. Manucharyan, “High-coherence fluxonium qubit,” *Phys. Rev. X* **9**, 041041 (2019).
- ¹¹ A. Whittaker, A. Y. Smirnov, T. Lanting, J. Whittaker, T. Medina, et al., “Probing flux and charge noise with macroscopic resonant tunneling,” (in preparation).